Journal of Physics: Conference Series

PAPER • **OPEN ACCESS**

Structure analysis of the thermal energy spectrum generated during stimulation of organic matter by an electromagnetic field

To cite this article: E Popardowski *et al* 2021 *J. Phys.: Conf. Ser.* **1782** 012028

Structure analysis of the thermal energy spectrum generated during stimulation of organic matter by an electromagnetic field

E Popardowski[1], P Kiełbasa[1], T. Dróżdż[1] and M Rad[2]

[1]Department of Machinery Exploitation Ergonomics and Production Processes, University of Agriculture in Krakow, Balicka 116B, 30-149 Krakow, Poland
[2]Department of Power Electronics and Energy Control Systems, AGH University of Science and Technology, Al. Mickiewicza 30, 30-059 Krakow, Poland

Abstract. The article presents the spectral characteristics of the temperature distribution in an induction coil which is an actuator in the technology of electromagnetic stimulation of organic matter and in the technology of elimination of undesirable microorganisms. The rate and method of heating the coil were precisely determined depending on the magnitude of the magnetic induction and the stimulation time of the material as well as the amount of flow of the coil cooling agent. Based on the experiment, the structure of the exposure time and the structure of the distribution of biological material in the working part of the coil were determined. Furthermore, the degree of cooling was determined so as to eliminate the uncontrolled momentary temperature amplitude on the course of the organic matter stimulation process.

1. Introduction

Determining the structure of the thermal energy spectrum is most often done using a technology called thermography. It is based on the use of special cameras that enable the determination of the value of the emitted infrared radiation and its visualization within the tested object. The generated image is a representation of the temperature distribution. The use of thermal imaging cameras in technology, initially limited to assessing the energy efficiency of buildings [1-3], was later extended, among others for non-invasive detection of objects and devices for electrical installations [4,5], including renewable energy devices [6,7], detection of unmanned aerial vehicles [8], or for the analysis of thermal processing of materials [9-12].

It seems particularly important to determine the heat energy distribution in relation to organic substances intentionally exposed to the electromagnetic field. In such systems, according to the Joule-Lenz law [13], a significant amount of heat is generated, which in many cases may be a factor determining the effect caused by stimulation, and thus limiting the influence of electricity itself on the tested object. The analysis allows for the identification and elimination of undesirable effects caused by exceeding the limit temperature leading to the destruction of biological structures. For organic material, the thermal denaturation process begins at a temperature (depending on the type of amino acid) from 40°C for myosin to 76°C for actin [14]. This range is wide, and the obtained values depend, apart from the type of the protein itself, on the kinetics of heating [15], or its earlier processing [16-18], as well as the pH [19,20]. However, it has been documented that under certain circumstances (increased heating rate and a selected type of protein) this temperature may be as low as 35°C [21]. It seems, therefore, that the determination of the thermal energy spectrum using thermovision during the stimulation of organic matter with an electromagnetic field may bring a twofold benefit, resulting both from extending the life of the apparatus, by identifying and then limiting excessive heating of working elements, and control of the temperature achieved by material, in order to eliminate conditions that may cause changes in the biological structure of the matter.

2. Materials and methods

The aim of the research was to determine the structure of thermal energy generated by the stand for stimulating organic matter with an electromagnetic field, taking into account various combinations of field voltage and device operation time, as well as the efficiency of the coil cooling system. The tests were carried out on a measuring stand [22], that the working element of which was a solenoid with a forced cooling system, where the cooling agent was water. The length of the coil was 480 mm, and the diameter of the exposure area was 60 mm (figure 1).

Figure 1. Actual view of the organic matter stimulation coil.

The device is powered by a specially designed transformer powered by 230 V, 15 kVA at 50 Hz. The transformer on the secondary side has the ability to supply the inductor with various currents and, consequently, to change the electromagnetic induction inside the solenoid by changing the magnitude of the current flowing through the coil winding according to equation 1,

$$B=(\mu_0 \cdot n \cdot I)/L \ [T] \tag{1}$$

where: B - induction in the solenoid [T], μ_0 - magnetic permeability of the vacuum, n - number of turns of the solenoid, I - current supplying the solenoid [A], L - solenoid length [m]

The interconnection of two factors: magnetic induction and stimulation time allows to determine the influence of both parameters on the course of the electromagnetic field influence. The concept of exposure dose was introduced as a measure linking the two parameters, which makes it possible to compare successive combinations of electromagnetic induction and time while maintaining a constant dose according to equation 2

$$D=10^7/4\pi \cdot B^2 \cdot t_e \ \ [J \cdot m^{(-3)}] \tag{2}$$

where: B-magnetic induction [T], t_e - exposure time [s].

The tests were carried out for three induction combinations, i.e. 20 mT, 40 mT and 70 mT, where in the first phase of the experiment the same amount of refrigerant was used equal 0.04 $l \cdot s^{-1}$. The volume of refrigerant was increased to 0.07 $l \cdot s^{-1}$ only for an induction of 70 mT. The heating characteristics of the coil's actuators were recorded with a TG275 ™ type thermal imaging camera from the coil switching on until the standard stimulation conditions for organic matter were reached. The camera lens was positioned centrally on the coil winding, the material of which was uniformly, which eliminated the influence of the inhomogeneity of the reflection coefficient on the infrared image indications. The thermal image was archived every 15 seconds. Temperature indications resulting from the infrared image were verified with a pyrometer, which measured the temperature on the surface of the coil winding along the symmetry of its transverse axis at intervals of 10% of the working coil length.

3. Results

Stimulation of biological material is a process whose parameters must be precisely maintained for the desired effect of the operation to be acceptable. One of the factors that may disturb the stimulation process is the temperature of the coil winding during operation. Biological substances are very sensitive to its fluctuations during stimulation, therefore its value should be controlled and planned in order to strengthen the stimulation in some substances and minimize it in others. Figure 2 shows the temperature distribution of the coil winding in selected periods of its operation with a magnetic induction of 20 mT.

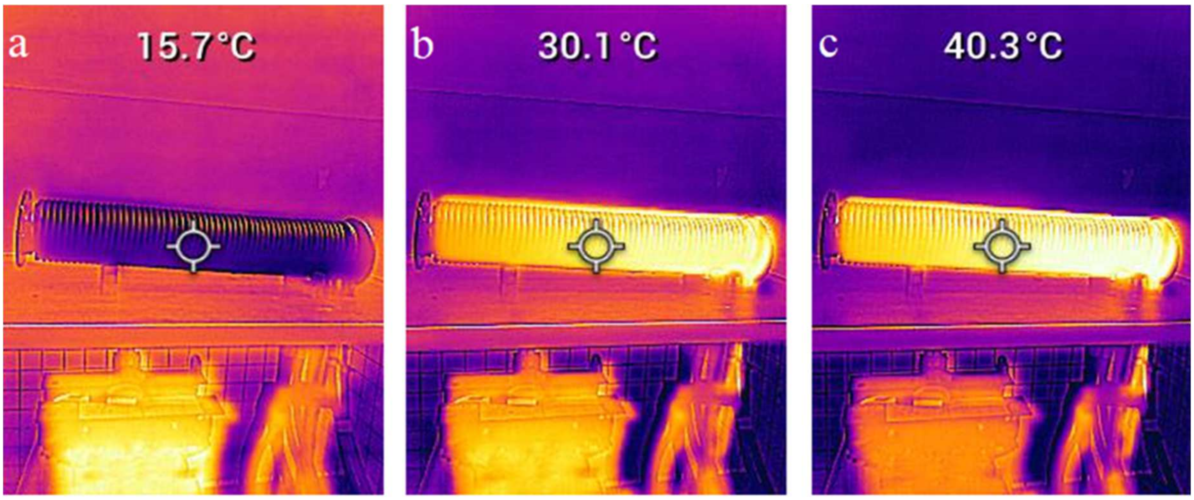

Figure 2. Visualization of the temperature distribution of the coil winding (20 mT): a - at the beginning of operation, b - after ten minutes of operation, c - after twenty minutes of operation.

The temperature of the coil winding at the beginning of its operation (figure 2a) was identical to the temperature of the cooling medium and was 15.7°C, the flow volume of which was 0.04 l·s-1. The temperature distribution was even, adequate to the constructed cooling system. At the set parameters, after 10 minutes of operation, the coil winding temperature increased to 30.1°C and it was noticed that its distribution was uneven (figure 2b). A much higher temperature was recorded at the point of exit of the cooling liquid nozzles. It is the result of its heating during the flow through the coil winding, and the placed pipes introducing the cooling medium into the system in the same place did not compensate for the increase in temperature of the medium leaving the system. After 20 minutes of operation, the coil winding temperature increased to 40.3ºC and its distribution was also uneven and in the part where the stub-tube were terminated, the temperature significantly exceeded 42.0ºC, which may cause protein denaturation during stimulation. The section of the coil at this temperature should be eliminated from the stimulation of organic matter, but it can be used in other processes, or the residence time of the biological material in this place of the coil should be limited. Maintaining the cooling medium flow volume of 0.04 l·s-1, but increasing the induction to 70 mT, it was found that the coil winding reached the temperature of 30ºC only 4 minutes after switching on (figure 3b). It should be noted that the initial temperature was 16.1ºC (figure 3a). The temperature distribution was similar to the induction of 20 mT, but the temperature gradient was much higher.

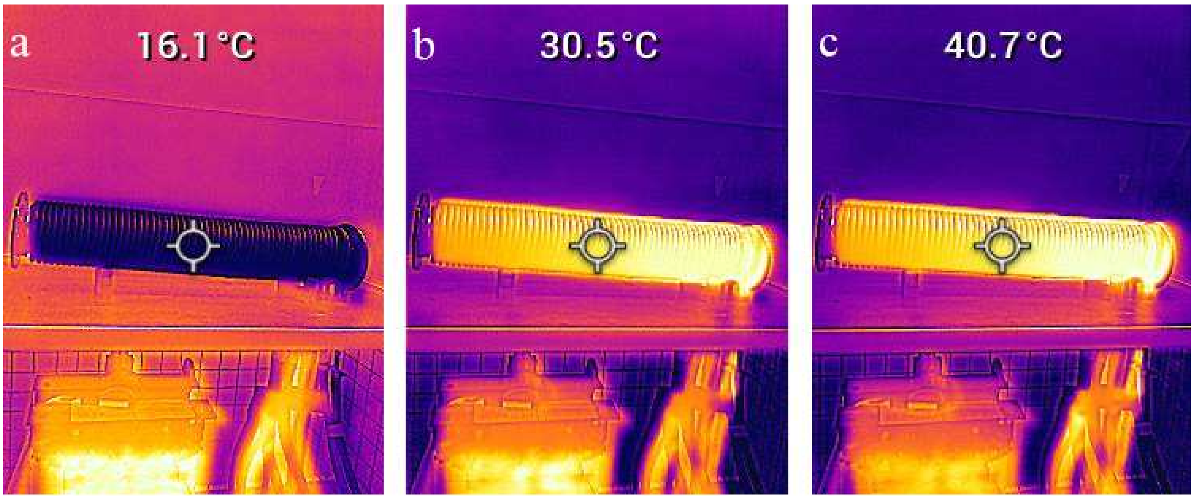

Figure 3. Visualization of the temperature distribution of the coil winding (70 mT): a - at the beginning of work, b - after fifteen minutes of work, c - after twenty minutes of work.

The coil winding reached the temperature of 40ºC after 15 minutes of operation, and the structure of temperature variation corresponded to the direction of the cooling medium flow, therefore it was the highest in the place where the stub-tube were placed. The identified structure of the temperature distribution within the coil winding allows for its purposeful use during the movement of the stimulated material to intensify the substance reaction to the influence of the electromagnetic field. In the case of using an induction of 90 mT, the heating time was even faster, and the temperature distribution characteristics were similar to those already described. After the volume of the cooling medium flow was increased to 0.07 l·s-1 for the analyzed coil with an induction of 90 mT, the temperature distribution is shown in figure 4.

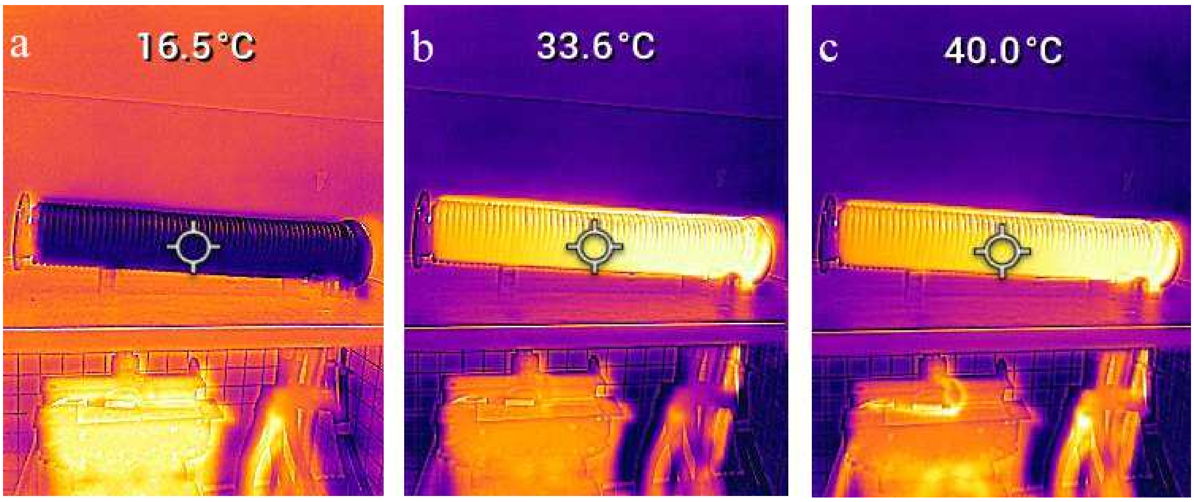

Figure 4. Visualization of the temperature distribution of the coil winding (90 mT): a - at the beginning of work, b - after ten minutes of work, c - after eighteen minutes of work.

The almost doubled volume of the cooling medium flowing through the coil cooling system extended the heating time of its winding to 18 minutes in the case of reaching the temperature of 40°C compared to the heating time recorded for the induction of 70 mT, where this time was 15 minutes. The temperature distribution within the coil winding was similar to the temperature distribution in the case of lower induction values.

4. Conclusion

The analysis of the thermal energy spectrum structure generated during the stimulation of organic matter with an electromagnetic field turns out to be extremely useful for the elimination of undesirable effects caused by exceeding the limit temperature, and thus the destruction of biological structures. The use of a thermal imaging camera for this purpose allows for precise and accurate determination of the place and time when the stimulated sample should be removed from the station. In addition, the control of the generated thermal energy allows the exclusion of the temperature factor as not parameterized in the final effect of stimulation. The knowledge of the characteristics of the thermal spectrum in the working space of the coil allows to model the stimulation process with a temperature variable.

References

[1] Preda A Lelia-Letitia P and Razvan S P 2018 Increasing comfort in a building using thermography *Proc. Int. Conf. on Advanced Topics in Optoelectronics, Microelectronics, and Nanotechnologies IX* vol 10977 (Constanta) p 4
[2] Daffara C Muradore R Piccinelli N Gaburro N Rubeis T and Ambrosini D 2020 A cos-effective system for aerial 3D thermography of buildings *J. Imaging* **6**(8) 76
[3] Huang Y Shih P Hsu K T and Chiang C H 2020 To identify the defects illustrated on building facades by employing infrared thermography under shadow *NDT E Int.* **111** 102240
[4] Dutta T Santra D Peng-Lim C Sil J and Chottopadhyay P 2019 Statistical Feature Analysis of Thermal Images from Electrical Equipment *Decision Science in Action. Asset Analytics (Performance and Safety Management).* eds Deep K, Jain M and Salhi S (Singapore: Springer) chapter 10 pp 127-137
[5] Esenboga B and Demirdelen T 2020 Efficiency and cost based multi-optimization and thermal/electromagnetic analyses of 3-phase dry-type transformer *IETE Journal of Research* **66**(4)
[6] Saginov L D 2016 Thermovision-thermografic research of local current density distribution over the area of PV cells *Int. J. of Applied Eng. Research* **9**(11) pp 6151-54
[7] Cubukcu M and Akanalci A 2020 Real-time inspection and determination methods of faults on photovoltaic power systems by thermal imaging in Turkey *Renewable Energy* **147**(1) pp 1231-38
[8] Sosnowski T Bieszczad G Madura H and Kastek M 2018 Thermovision system for flying objects detection *Symp. of Baltic URSI* (Poznan) pp 141-144
[9] Piecuch G Madera M and Żabiński T Diagnostics of welding process based on thermovision images using convolutional neural network *IOP Conf. Series: Materials Science and Engineering* **710**
[10] Cojocaru R Botila L N and Ciuca C 2020 Infrared thermographic technique – viable alternative for monitoring of friction processing processes *Welding & Material Testing* **1**(20) pp 3-9
[11] Korzeniewska E, Szczesny A, Krawczyk A, Murawski P, Mroz J, Seme, S 2018 Temperature distribution around thin electroconductive layers created on composite textile substrates, *Open Physics*, 16 (1) 37-41
[12] Swiatczak T, Tomczyk M, Wiecek B, Pawlak R, Olbrycht R, 2012 Defect detection in wire welded joints using thermography investigations, *Materials Science And Engineering B-Advanced Functional Solid-State Materials,* 177 (15) 1239-1242
[13] Olszewski S 2016. Conservation of energy in classical mechanics and its lack from the point of view of quantum theory *J of Mod Phys* **7** pp 2316–28
[14] Skipnes D Van der Plancken I Van Loey A and Hendrickx M 2008 Kinetics of heat denaturation of proteins from farmed Atlantic cod (Gadus morhua) *J of Food Eng* **85**(1) pp 51-58
[15] Ovissipour M Rasco B Tang J and Sablani S 2017. Kinetics of Protein Degradation and Physical

Changes in Thermally Processed Atlantic Salmon (Salmo salar) *Food and Bioprocess Technology* **10** pp 1865-82

[16] Jin Y Liang R Liu J Lin S Yu Y and Cheng S 2017 Effect of structure changes on hydrolysis degree, moisture state, and thermal denaturation of egg white protein treated by electron beam irradiation *LWT - Food Science and Technology* **77** pp 134-141

[17] Jakubowski T 2020 The effect of stimulation of seed potatoes (Solanum tuberosum L.) in the magnetic field on selected vegetation parameters of potato plants *Przeglad Elektrotechniczny* **96** pp 166-169

[18] Jakubowski T 2019 A system for the control and recording of physical parameters inside a chamber for UV-C irradiating of biological material *Proc. Int. Conf. POLSITA 2019 Progress of mechanical engineering supported by information technology* vol 132 (Czajowice) 01006

[19] Rios-Mera J D Da Silva Pinto J S and Contreras-Castillo C J 2017 Effect of ultimate pH and ageing on thermal denaturation of bovine muscle proteins *Meat Science* **131** pp 25-7

[20] Leeb E Haller N and Kulozik U 2018 Effect of pH on the reaction mechanism of thermal denaturation and aggregation of bovine β-lactoglobulin *International Dairy Journal* **78** pp 103-111

[21] Llave Y Shibata-Ishiwatari N Watanabe M Fukuoka M Hamada-Sato N and Sakai N 2018 Analysis of the effects of thermal protein denaturation on the quality attributes of sous-vide cooked tuna *Journal of Food Proc and Pres* **42**(1)

[22] Drozdz T Bienkowski P Kielbasa P Nawara P and Popardowski E 2019 The research stand to stimulation of biological materials by the various electromagnetic field *Przegląd Elektrotechniczny* **95** pp 66-69